RESEARCH PAPER
https://doi.org/10.1071/EN23013

Environmental Chemistry

Molecular composition and the impact of fuel moisture content on fresh primary organic aerosol emissions during laboratory combustion of ponderosa pine needles

Mohammed Jaoui[A,*], Shawn P. Urbanski[B], Russell W. Long[A] and Matthew S. Landis[A]

Environmental context. Wildland fire smoke and its impacts on air quality and human health are increasing globally. However, uncertainties in organic emissions from these fires hinder our understanding of downwind atmospheric photochemical processes driving the formation of hazardous air pollutants. In this study, we investigated the impact of fuel moisture content on organic species emission during the combustion of ponderosa pine needles, an important fuel source in the western United States.

For full list of author affiliations and declarations see end of paper

***Correspondence to:**
Mohammed Jaoui
US Environmental Protection Agency (EPA), Office of Research and Development, Research Triangle Park, NC, USA
Email: jaoui.mohammed@epa.gov

Handling Editor:
Zongbo Shi

ABSTRACT

Rationale. Pine needles represent an important fuel source in coniferous forest systems in the western United States. During forest fires, they can be easily ignited and help sustain flame on the ground. **Methodology.** In this study, a comprehensive chemical analysis was conducted to examine oxygenated organic compounds (OOCs) present in $PM_{2.5}$ (particles ≤ 2.5 μm in aerodynamic diameter) formed from burning dry and moist ponderosa pine (*Pinus ponderosa*) needles (PPN) in the presence and absence of fine woody debris (FWD). The effect of fuel moisture content (FMC), a key parameter that influences smoke formation, has not received much attention. Therefore, we also investigated the effect of FMC on $PM_{2.5}$ formation and its composition. Thirty three experiments were conducted at the US Forest Service Fire Science Laboratory. $PM_{2.5}$ was collected onto 47-mm Teflon filters, and silylated extracts were analysed by gas chromatography–mass spectrometry. **Results.** More than 50 OOCs were identified, including levoglucosan and mannosan; *n*-dodecanoic acid and *n*-hexadecanoic acid; dihydroabietic acid, and dehydroabietic acid; and a series of intermediate volatile and semivolatile organic compounds. Mass spectra of a wide variety of compounds in electron and chemical ionisation mode are provided. Most of these OOCs were identified in this study for the first time in PPN aerosol, although some were previously reported in pine wood and other biomass burning aerosol. Our results show significant changes in the composition and abundance of particles depending on the amount and type of PPN burned. When compared with dry PPN, moist PPN showed decreased emissions of $PM_{2.5}$ and OOCs, due likely to the presence of water in the system that partially suppressed the production of OOCs. **Discussion.** Incorporating pine needles in atmospheric models as a contributor to smoke particles generated during forest fires is an essential step towards reducing the current uncertainties regarding the influence of these aerosols on chemical/air mass characteristics, regional meteorology, and the climate.

Keywords: diterpenoids, organic aerosol, oxygenated organic compounds, $PM_{2.5}$, ponderosa pine needles, silylation, sugars, wildfires, wildland fire smoke.

Received: 30 January 2023
Accepted: 10 December 2023
Published: 22 January 2024

Cite this:
Jaoui M *et al.* (2023)
Environmental Chemistry
20(8), 319–338. doi:10.1071/EN23013

Introduction

Wildfires are unplanned and uncontrolled fires that start in wildland areas but often spread to populated areas. Over the past few decades, the frequency, size, duration, and severity of wildfires and the associated impacts on air quality have increased across many regions of the globe (Bowman *et al.* 2009, 2011; Stephens *et al.* 2013; Westerling 2016; Balch *et al.* 2017; Holden *et al.* 2018; Landis *et al.* 2018). Recently, the United States, particularly the West, has experienced some of the largest and most damaging wildfires

in decades (Holden *et al.* 2018), and fires are expected to increase in size and intensity in the future due to the changing climate, drought, and increased urbanisation and development (Westerling *et al.* 2006; Bowman *et al.* 2009, 2011; Stephens *et al.* 2013; Liu *et al.* 2016; Westerling 2016; Balch *et al.* 2017; Holden *et al.* 2018). Recent studies show that total U.S. particulate matter (PM) air quality continues to improve except in areas affected by wildfires (McClure and Jaffe 2018*a*, 2018*b*). Wildfires can impact air quality and influence climate at local, regional, and even global scales (Westerling *et al.* 2006; Westerling 2016; Malig *et al.* 2021).

Smoke from wildland fires is composed of a wide variety of gases: carbon monoxide (CO), carbon dioxide (CO_2), volatile organic compounds (VOCs), and oxides of nitrogen (NOx) (Simoneit 2002; Vicente *et al.* 2013; Urbanski 2014; Hatch *et al.* 2015). Wildfires also directly emit a large amount of $PM_{2.5}$ (particles $\leq$ 2.5 μm in aerodynamic diameter), a criteria air pollutant regulated under the U.S. Clean Air Act (42 U.S. Code § 7409), as amended (1990). Recently wildfires were estimated to account for 25% of $PM_{2.5}$ across the United States, and up to 50% in some western regions (Burke *et al.* 2021). The type of fuels (e.g. live and dead biomass available for combustion – litter, down dead wood, organic soil, herbs, shrubs, and the foliage and fine branch wood of tree crowns) being burned has a strong influence on the chemical composition of the smoke produced (Urbanski 2014; Baylon *et al.* 2015; Briggs *et al.* 2016). Although VOCs, semivolatile organic compounds (SVOCs), and nonvolatile organic compounds can be emitted directly into the atmosphere during wildfires, VOCs and SVOCs can also react further with atmospheric oxidants like hydroxyl radicals during the day and nitrate radicals at night. Additionally, VOCs and SVOCs can react with ozone at any time to yield additional SVOCs and nonvolatile products that partition into particles, forming secondary organic aerosol (SOA) (Nozière *et al.* 2015; McClure and Jaffe 2018*b*).

$PM_{2.5}$ is one of the main pollutants the public is exposed to for short periods of time (hours to weeks) during wildfires. $PM_{2.5}$ from biomass burning contributes significantly to the global atmospheric organic aerosol (OA) burden (Crutzen and Andreae 1990; Bond *et al.* 2004). $PM_{2.5}$ is composed of a variety of chemical species, each with their own sources, physio-chemical properties, atmospheric reaction pathways, and environmental impacts. Pine forests, which dominate several areas of the globe, including northern parts of North America, Europe, and Russia, contribute significantly to biomass burning particles (Liang *et al.* 2021, 2022). Most studies associated with pine trees focused on the estimation of biogenic reactive organic compounds (e.g. pinene compounds: α-pinene and β-pinene) and their contribution to the atmospheric carbon budget and the production of tropospheric ozone and aerosol particles (Guenther 2002; Nozière *et al.* 2015). For the characterisation of smoke associated with pine needle burning, most studies reported on emissions of CO, CO_2, NOx, elemental and organic carbon (EC and OC), and PM, with few reporting on OA characterisation (Laskin *et al.* 2009). Laskin *et al.* (2009) established that OC was the main component of aerosols, and have reported a new class of chemicals, N-heterocyclic alkaloids, emitted from burning ponderosa pine (*Pinus ponderosa*) needles (PPN), sticks, and duff. When released into the atmosphere, these chemicals can partition into particles and be transported hundreds to thousands of kilometres, which may directly impact the health of humans and animals, and be atmospherically deposited and mobilise into surface and groundwater systems (Bladon *et al.* 2014; Jen *et al.* 2019). Recently, based on chamber burns of 19 different species including pine needles, oxygenated aerosol was found to contribute to the OA emitted based on the m/z 44 fragment measured by the aerosol mass spectrometer (Jolleys *et al.* 2014). Overall, the composition, chemical transformation, and sources of OA are currently not well characterised for biomass burning including OA from pine needles. Most studies have used either the emission factors (EF) and/or the modified combustion efficiency (MCE; Urbanski 2013) to evaluate the OA contribution from fires. OA composition and emissions factors of anhydrous sugars and other organic components have been reported previously (Nolte *et al.* 2001; Oros and Simoneit 2001; Schauer *et al.* 2001; Hosseini *et al.* 2013; Jen *et al.* 2019) from the burning of wildland fuels. These results revealed that aerosols originating from biomass burning are far from uniform. Furthermore, better chemical and physical characterisation of aerosols from different combustion sources is an essential step towards reducing the current uncertainties regarding the influence of these aerosols on chemical/air mass characteristics, regional meteorology, and the climate (Jolley *et al.* 2012, 2014).

The present study is part of a larger U.S. Environmental Protection Agency (EPA) Wildland Fire Sensor Challenge conducted by the EPA and the U.S. Forest Service (USFS), in collaboration with other U.S. federal agencies (Centers for Disease Control and Prevention (CDC); National Aeronautics and Space Administration (NASA); National Oceanic and Atmospheric Administration (NOAA); National Park Service (NPS)) to evaluate the performance of new air measurement technologies for monitoring wildland fire smoke (Landis *et al.* 2021). Here, our focus is conducting a comprehensive qualitative and quantitative chemical analysis of OOCs bearing –OH and –COOH groups from $PM_{2.5}$ smoke samples collected during the 2018 phase two of the U.S. EPA Wildland Fire Sensor Challenge (Landis *et al.* 2021). Smoke was generated under simulated wildland fire conditions at the USFS Fire Sciences Laboratory (FSL) combustion chamber in Missoula, Montana (Christian *et al.* 2004). Varying concentrations of smoke from burning PPN at two moisture levels, dry and moist, in the presence and absence of ponderosa pine fine woody debris (FWD, downed, dead twigs, and small (diameter $<$ 1.5 cm) branches) were produced in the chamber. Thus, the effects of the composition of the fuel

burned on the variability in emissions of oxygenated organic compounds (OOCs) is evaluated. In particular, the roles of combustion processes, source conditions such as fuel type and morphology, and oxygenation levels of resulting OA are of interest. An analytical method coupling gas chromatography to mass spectrometry (GC-MS) with a derivatisation method (silylation) (Jaoui *et al.* 2004) has been used for the identification of OOCs originated from samples obtained from chamber experiments.

Experimental

Chamber description and operation

While the organic species associated with the combustion of PPN can be found in field samples collected during wildland fires in areas dominated by pine trees, they are most readily formed and identified by laboratory burn experiments. The initial conditions of the combustion experiments conducted in this study are summarised in Table 1. Thirty-three experiments were conducted from 16 to 24 April 2018, 16 with PPN and 17 with a mixture of PPN and FWD. The experiments were carried out under conditions that mimic the types of atmospheric combustion likely to occur under typical ambient conditions.

All burn experiments were carried out at the combustion chamber at the USFS FSL. The FSL combustion chamber has a volume of ~3000 m^3 with internal dimensions 12.4 × 12.4 × 19.6 m^3 (L × W × H). Additional chamber details can be found elsewhere (Christian *et al.* 2004). The chamber was operated in 'static' mode where prior to each burn the chamber was flushed with outdoor ambient air and then sealed by closing the exhaust stack prior to fire ignition. Two large circulation fans mounted on the wall of the chamber and destratification fans on the chamber ceiling facilitated mixing and maintained homogeneous smoke conditions (Landis *et al.* 2021). Fuel beds were prepared and placed in the centre of the chamber (see below). The fuel beds were ignited, and smoke sampling commenced after both flaming and smouldering combustion had ceased and the smoke concentration within the chamber had stabilised. Based on a recent study of particle wall-loss in smog chambers, we believe particle wall-loss is small (<10%) during our 1 h tests. Wang *et al.* (2018) found wall-loss rates in a 12 m^3 Teflon chamber to be 0.1 h^{-1} for 100 nm and 0.25 h^{-1} for 50 nm particles. Given the much larger volume of the FSL combustion chamber (3000 m^3), we anticipate the particle loss rate to be substantially less than that for the 12.5 m^3 chamber evaluated in Wang *et al.* (2018). In addition to chamber size, the electrostatic effect, which will be enhanced for Teflon walls, can play a major role in increasing wall-loss of intermediate size particles (0.5 nm–1 μm) (McMurry and Rader 1985). Since the walls of the FSL combustion chamber are lined with corrugated aluminium, the particle wall-loss rate should be further reduced compared with that reported in Wang *et al.* (2018). For each burn, smoke was sampled for 1 h. A total of 33 burns were performed from 16 to 24 April 2018 under different burn conditions resulting in 33 1-h filter sample periods. While the focus has been to qualitatively examine the particle phase composition of OOCs, measurements of trace gas phase species and other parameters (e.g. EC and OC) have been also made. Real-time trace gas measurement of NO (nitric oxide), NO_2 (nitrogen dioxide), O_3, CO_2, CO,

Table 1. Summary of initial conditions associated with the 33 burn experiments conducted at the FSL chamber, Missoula, Montana, April 16–24, 2018 (see Supplementary Table S1).

Conditions				
	Total	Dry	Moist	Dry + Moist
Fuel type		Ponderosa pine needles (PPN)		
Number of burns	16	2	5	9
Total fuel mass (g): min–max	20–779	20–779	90–355	22–84 + 16–218
Moist/dry ratio: min–max	0.6–5.1	–	–	0.6–5.1
Fuel type	Ponderosa pine needles (PPN) + fine pine woody debris (FWD)			
Number of burns	17	15	1	1
Total fuel mass (g): min–max	10–700 (PPN)	10–700 (PPN)	171 (PPN)	40 (dry PPN)
	21–2230 (FWD)	21–2230 (FWD)	118 (FWD)	34–38 (moist FWD)
		21–2230 (FWD)		
Moist/dry ratio: min–max	1.8[A]	–	–	1.8[A]
PPN/FWD ratio: min–max	0.03–2.4	0.03–2.4	1.1	2.0[B]

[A]Moist (PPN + FWD)/dry PPN (burn #25, Supplementary Table S1).
[B]Dry PPN/moist FWD (burn #25, Supplementary Table S1).

and SO_2 (sulfur dioxide) were made for each burn experiment using commercial gas analysers, and can be found elsewhere (Landis *et al.* 2021).

Fuels

The present study investigates the chemical composition of smoke generated in the chamber to simulate near- to mid-field wildland fire smoke conditions (Landis *et al.* 2021). Varying concentrations of smoke were generated from burning biomass typical of the Western U.S. under various combustion conditions (e.g. smouldering, flaming). The fuels used were PPN and ponderosa pine FWD (downed, dead twigs, and small diameter (<1.5 cm) branches). Both 'dry' and 'moist' fuels were used and the mass fraction of FWD in the fuel beds ranged from 0 to >95%, see Supplementary Table S1. The chamber temperature, relative humidity, and initial fuel mass (dry weight) of PPN and FWD burned in each experiment are summarised in Supplementary Table S1.

Particle sampling

Particle samples ($PM_{2.5}$) from the chamber were collected onto 47 mm polytetrafluoroethylene (PTFE) filters at 1 $m^3 h^{-1}$ for 1 h, using three Tisch Environmental (Cleves, OH, USA) Model TE-WILBUR filter-based U.S. EPA Federal Rerence Method (FRM) samplers distributed in the burn chamber. Three FRM sampler filters were collected from each burn. Each Tisch sampler used a standard EPA PM_{10} (particles with aerodynamic diameters ≤10 µm) louvered impactor inlet and $PM_{2.5}$ fractionation was performed by a BGI by Mesa Labs (Butler, NJ, USA) Model VSCCA (Very Sharp Cut Cyclone). The samplers were programmed to start 10–15 min after fuel ignition to allow for the combustion of the fuel beds, flame out, and mixing of the smoke. Measurement Technology Laboratories (MTL; Minneapolis, MN, USA) Model PT47P PTFE 2 µm pore size pressure drop equivalent membrane filters, with a hydro-inert fluorinated ethylene propylene (FEP) support ring from the same lot, were used in every sampler. Filters were weighed in accordance with EPA Guidance Document 2.12 (U.S. EPA 2016) for monitoring $PM_{2.5}$ in ambient air. Before and after sampling, filters were equilibrated for a minimum of 24 h in a temperature and humidity controlled clean room prior to being weighed by an MTL Model AH1 Automated Weighing system. Filter weights were performed in triplicate and were accepted as valid if they were within ±5 µg of each other. Final weights were calculated from the mean of the triplicate readings. A detailed description of the samplers, filters, and sampler calibration procedure can be found elsewhere (Krug *et al.* 2021; Landis *et al.* 2021).

Sample extraction and derivatisation

The following chemicals were purchased from Aldrich Chemical Co. (Milwaukee, WI, USA): 1,2-decanediol, 1,12-dodecanediol, pentadecane dioic acid, 11-hydroxyundecanoic acid, 16-hydroxyhexadecanoic acid, 9-hydroxynonanoic acid, 1,14-tetradecanediol, palmitic acid, 1,10-decanediol, 1,2-dodecanediol, 1,9-nonanediol, 7-oxononanoic acid, hexadecanedioic acid, 1,16-hexadecanediol, 15-hydroxypentadecanoic acid, 1,4-anhydroerythritol, D-erythronic acid-γ-lactone, 2-hydroxy-5-methylacetophenone, DL-threitol, methyl-β-D-xylopyranoside, phthalic acid, levoglucosan, xylose, D-arabitol, isophthalic acid, sorbitol, D-mannitol, galactosan, inositol, tetracosane-d_{50} (TCS: IS), (1*S*)-(+)-ketopinic acid (KPA: IS), *trans*-*p*-menth-6-ene-2,8-diol (PMD: IS), and *N*,*O*-bis(trimethylsilyl)trifluoroacetamide (BSTFA). Mass spectra were generated for these chemicals and used to help interpret the mass spectra associated with products that originated from smoke particles. All compounds were purchased at the highest purity available and were used without further purification. Methylene chloride, acetone, hexane, *n*-pentane, and acetonitrile were of GC^2 quality, and were purchased from Burdick and Jackson (Muskegon, MI, USA).

Filter samples from the chamber were sonicated for 1 h in 3 mL of methanol/methylene chloride (1:1, v/v). Each filter was placed in a clean 5 mL conic-bottom tube with a Teflon-lined cap. Prior to extraction, 20 µL each of KPA (58.1 µg mL^{-1}), PMD (100.2 µg mL^{-1}), and TCS (56.9 µg mL^{-1}) were spiked on the top of the filter as internal/recovery standards, then 3 mL of the extraction solvent was added. The tube was capped and sonicated for 1 h at room temperature. After cooling at room temperature for 15 min, each sample extract was evaporated to dryness under a gentle stream of ultrapure N_2 by using an N-Evap evaporation bath (Organomation Associates, Inc., Berlin, MA, USA). The resulting dry extract was then derivatised with 200 µL of BSTFA (*N*,*O*-bis- (trimethylsilyl)trifluoroacetamide/1% trimethylchlorosilane) and 100 µL of pyridine at 70°C for 1 h. After cooling to room temperature, the solutions were transferred to GC-MS vials and analysed by GC-MS in electron ionisation (EI) and methane chemical ionisation (CI) modes. EI is highly reproducible and fragmentation data are available for many compounds in mass spectral databases. Information about the molecular ion is often lost in EI because of the strong analyte fragmentation, which compromises the identification of unknown compounds. CI, on the other hand, offers the mass of the molecular analyte and its fragments, which is crucial when identification using EI fails due to insufficient library data and standard materials. For complex mixture analysis and to overcome these challenges, EI and CI are used as complimentary to each other, which boosts the confidence in the identification of unknown species, especially in complex mixtures as the case in this study. In some cases, depending on the concentration of each derivative, a dilution of 30% was made to avoid overloading the column (extracts from burns #9, #20, and #21). The extraction and derivatisation procedures were conducted using the method reported by Jaoui *et al.* (2004, 2018).

GC-MS analysis was conducted on an Agilent Technologies (Santa Clara, CA, USA) gas chromatograph – mass spectrometer instrument equipped with a model 7693-automatic sampler, a model 7890 B GC with a splitless injector, and a model 5977 B mass selective detector. An Agilent model DB-5MS capillary column (60 m, I.D. 0.25 mm, film thickness 0.25 μm) was used for the analysis. For these measurements, the inlet temperature was set to 280°C. The temperature program started at 84°C for 1 min and was raised first to 200°C at 10°C min^{-1} and then to 300°C at 30°C min^{-1}, where it was held for 5 min. Subsequently, 2 μL of the extract was injected in CI and/or EI modes. The MS was operated in full SCAN mode in EI (70 eV) and CI modes. The transfer line, source, and quadrupole temperatures were set to 280, 230, and 150°C, respectively.

Results and discussion

Experiments were conducted using moist and dry PPN and FWD. The moist/dry PPN and PPN/FWD mass ratio ranged from 0.6 to 5.1 and 0.03 to 2.4, respectively. Additional details associated with this study are provided in the Supplementary Material Table S1 and Landis *et al.* (2021). Chamber temperatures, relative humidity, and modified combustion efficiencies (MCEs) ranged from 22.5 to 26.9°C, 15.8–53%, and 0.911–0.971, respectively (Supplementary Table S1; Landis *et al.* 2021).

$PM_{2.5}$ concentrations associated with each burn are given in Supplementary Table S1 and ranged from 28.7 ± 7.4 μg m^{-3} to 1814.9 ± 265.3 μg m^{-3}. Overall, the $PM_{2.5}$ concentration was lowest in burn #5, corresponding to a fuel loading of 50 g of a mixture of dry PPN and FWD, and highest in burn #9, corresponding to a fuel loading of 779 g of dry PPN. The burn conditions (smouldering vs flaming), burn efficiency, MCEs, and gas phase species were provided and are discussed elsewhere (Krug *et al.* 2021; Landis *et al.* 2021). The production of smoke particles was found to be highly dependent on the conditions under which the burns were carried out, the presence or absence of moist PPN or FWD, and the total initial mass of fuel used (Supplementary Table S1). Fig. 1 displays the distribution of $PM_{2.5}$ (μg m^{-3}) concentration as a function of the initial mass of moist PPN used. $PM_{2.5}$ concentrations measured gravimetrically were highly correlated (r^2 = 0.97) with the mass of moist PPN burned (Fig. 1*a*). Note that only five data points are available for this regression. However, a consistent correlation was not observed when the fuel used was composed of a mixture of moist and dry PPN (r^2 = 0.25). A good correlation was also observed when the fuel burned is a mixture of PPN (moist) and FWD. In this case, the amount of $PM_{2.5}$ emitted increased with the mass of fuel burned (r^2 = 0.79). Fig. 1*b* displays emitted smoke $PM_{2.5}$ concentration (μg m^{-3}) versus the mass of initial PPN burned when mixtures of PPN and FWD were burned simultaneously. The data show that the fuel composition, in particular the PPN/FWD ratio, plays an important role in emitted $PM_{2.5}$ smoke levels. For low PPN to FWD ratios (~0.04), the amount of $PM_{2.5}$ emitted increased rapidly with the amount of FWD burned. For a high PPN to FWD ratio (~0.4), the amount of $PM_{2.5}$ increased moderately as the mass of PPN burned increased (Fig. 1*b*). When compared with dry PPN, moist PPN showed decreased emissions of $PM_{2.5}$ (e.g., from 140.9 μg m^{-3} (burn #4, Supplementary Table S1) to 45.8 μg m^{-3} (burn #18)), likely due to the production of $PM_{2.5}$ being partially suppressed in the presence of water in the system. This is consistent with the effect of relative humidity on SOA reported in the literature from the oxidation of isoprene (Nestorowicz *et al.* 2018). Therefore, fuel moisture content is an important parameter to understand because in the natural environment live fuels have elevated moisture content compared to dead dry fuel.

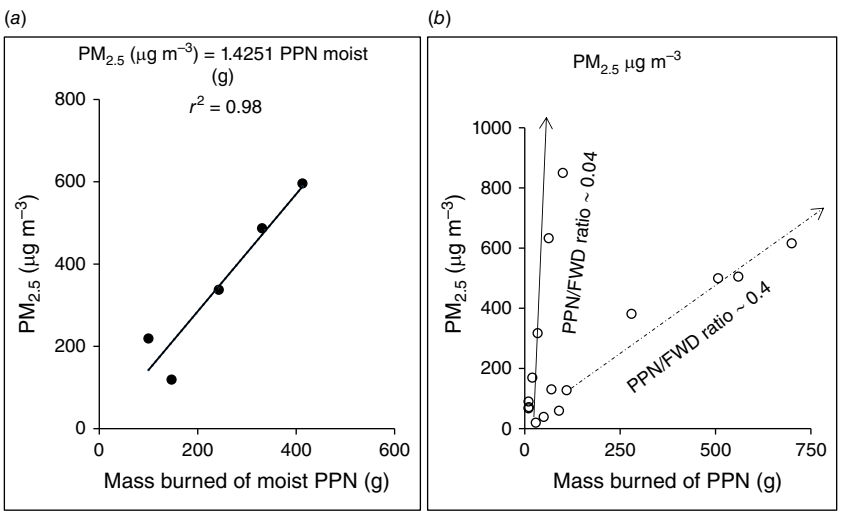

Fig. 1. $PM_{2.5}$ concentrations (μg m^{-3}) in the smoke chamber as a function of the mass of PPN burned (g). (*a*) $PM_{2.5}$ concentration versus initial mass of moist PPN used in the absence of FWD. (*b*) $PM_{2.5}$ concentration versus initial mass of PPN used in the presence of FWD. Solid line is the linear model least square regression (Fig. 1*a*).

Identification of oxygenated organic products

During each burn experiment, sufficient $PM_{2.5}$ mass was collected on PTFE filters to characterise select OOCs (Supplementary Table S1). The analysis of $PM_{2.5}$ generated from burning PPN and mixtures of PPN and FWD shows the presence of a series of organic compounds containing one or more of the following groups: ketone, ether, carboxylic acid, alcohol, and/or aromatic ring. Many of these compounds do not have authentic standards and their identification was based on the interpretation of mass spectra of the derivatised compound (Jaoui *et al.* 2004, 2005, 2018). The identification should be regarded as tentative except for compounds that have authentic standards. The recognition of characteristic ions was used to guide the analysis of the derivatives obtained in both EI and CI modes. BSTFA reacts with –COOH and –OH groups to form trimethylsilyl (TMS) derivatives, having characteristic fragment ions of *m/z* 73, 75, 147, and 149. Adduct ions in CI from the derivatives include *m/z* $M^{+\cdot}$ + 73/75, $M^{+\cdot}$ + 41, $M^{+\cdot}$ + 29, and $M^{+\cdot}$ + 1; fragment ions include *m/z* $M^{+\cdot}$ – 15, $M^{+\cdot}$ – 73, $M^{+\cdot}$ – 89, $M^{+\cdot}$ – 117, $M^{+\cdot}$ – 105, $M^{+\cdot}$ – 133, and/or $M^{+\cdot}$ – 207 (Jaoui *et al.* 2004). The approach used for the identification is as follows. Peaks detected in blank and/or background chamber samples were eliminated first. A peak was associated with a compound only if its corresponding mass spectrum was consistent with the fragmentation pattern of the BSTFA derivatisation reagent. All recorded spectra were compared with spectra derived from various reference compounds, authentic standards, NIST library, the PubChem website (pubchem.ncbi.nih.gov), mass spectra assignment, Gardner *et al.* (1999), Kononenko (2017), and Bankova *et al.* (2019). While the off-line technique is an integrated method that requires only 1 h sampling times, it still provides a sensitive method for product identification at the molecular level as well as measuring low concentrations of highly OOCs, including SVOCs and intermediate-volatile organic compounds (IVOCs). Thus, products found by this collection technique and analytical method could be informative for possible markers for the types of compounds that may form in smoke particles.

Fig. 2 displays typical GC-MS (portion 22–46 min) total ion chromatograms (TICs) associated with silylated extracts in EI mode. Mass spectra of more than 50 compounds have been recorded in the present study, for which representative examples are shown. Chromatograms for either EI or CI associated with $PM_{2.5}$ smoke indicated the presence of significant large peaks from the BSTFA derivatisation. They are best illustrated in Fig. 2 for dry PPN (14 peaks), moist PPN (11 peaks), and dry PPN + FWD (8 peaks). In addition, a significant number of relatively small peaks were detected in each chromatogram (Fig. 2). The structure of compounds associated with several peaks with mass spectra consistent with products bearing –OH and/or –COOH groups could not be obtained due to lack of authentic standards and the complexity of the interpretation of their spectra. Compounds identified in the present study are summarised in Table 2, which contains proposed structures, the five most abundant ions associated with each compound (CI) as a trimethylsilyl (TMS) derivative, and the molecular weights of the derivatised (MW_{TMS}) and underivatised (MW) compound. Additional peaks having mass spectra not consistent with silylation were detected and are associated with compounds not bearing –OH and –COOH groups (Table 2).

Sugars and sugar alcohols

Levoglucosan (LG: dioxabicyclo[3.2.1]octane-2,3,4-triol) was the highest concentration anhydrous sugar observed on all PPN (dry & moist) burn sample filters with a peak that eluted at 30.48 min in the chromatograms presented in Fig. 2*b–c* and field blank concentrations were typically non-detectable (Fig. 2*a*). When PPN was mixed with FWD, the observed levoglucosan concentrations were reduced (Fig. 2*d*). Supplementary Fig. S1 displays the mass spectrum of LG-3TMS in CI and EI recorded from a dry PPN sample, and the EI associated with the LG-3TMS standard. The EI mass spectrum (Supplementary Fig. S1*b*) shows strong TMS characteristic fragment ions at *m/z* 73, 204, 217, 147, 333, consistent with that recorded for the LG standard (Supplementary Fig. S1*c*) with a slight difference due to peak co-elution observed for that originated from the PPN sample. The corresponding CI spectrum also shows TMS fragment ions at *m/z* 317, 289, 273, 157, and 363 that are consistent with the EI mode and the presence of three –OH groups, indicating a TMS-derivatised molecular weight (MW_{TMS}) of 378 Da (all derivatised and underivatised masses are in Dalton (Da), but are not designated as such hereafter). Note, adducts ions in CI mode (e.g., *m/z* at ($M^{+\cdot}$ + 1), ($M^{+\cdot}$ + 29), and ($M^{+\cdot}$ + 41) were not observed for LG-3TMS (Supplementary Fig. S1*a*). LG has been widely used as a primary marker for biomass burning as it is formed during the thermal decomposition of cellulose and hemicellulose (Simoneit *et al.* 1999; Urban *et al.* 2014). Several additional sugars were identified in this study based on authentic standards including: mannosan (MN: 1,6-anhydro-β-D-mannopyranose) and galactosan (GL: 1,6-anhydro-β-D-galactopyranose) (Fig. 2, Table 2). MN and GL are detected at much lower concentrations than LG (Fig. 2), consistent with the work of Otto *et al.* (2006) and Liang *et al.* (2021). The LG/MN mass peak area ratios of 5.3, 8.3, and 13.2 associated with burn #9, #28, and #14, respectively, were consistent with those reported for aerosol samples (Decesari *et al.* 2006; Kundu *et al.* 2010; Xu *et al.* 2019; Hou *et al.* 2021), and particulate material emitted during burning various types of wood (Gonçalves *et al.* 2011). The LG/MN mass ratio is used to differentiate between burning softwood (low ratio) and hardwood (high ratio) (Cheng *et al.* 2013). This is consistent with our results showing a higher LG/MN ratio for burns involving FWD (burn #14) and a lower LG/MN ratio for burns involving

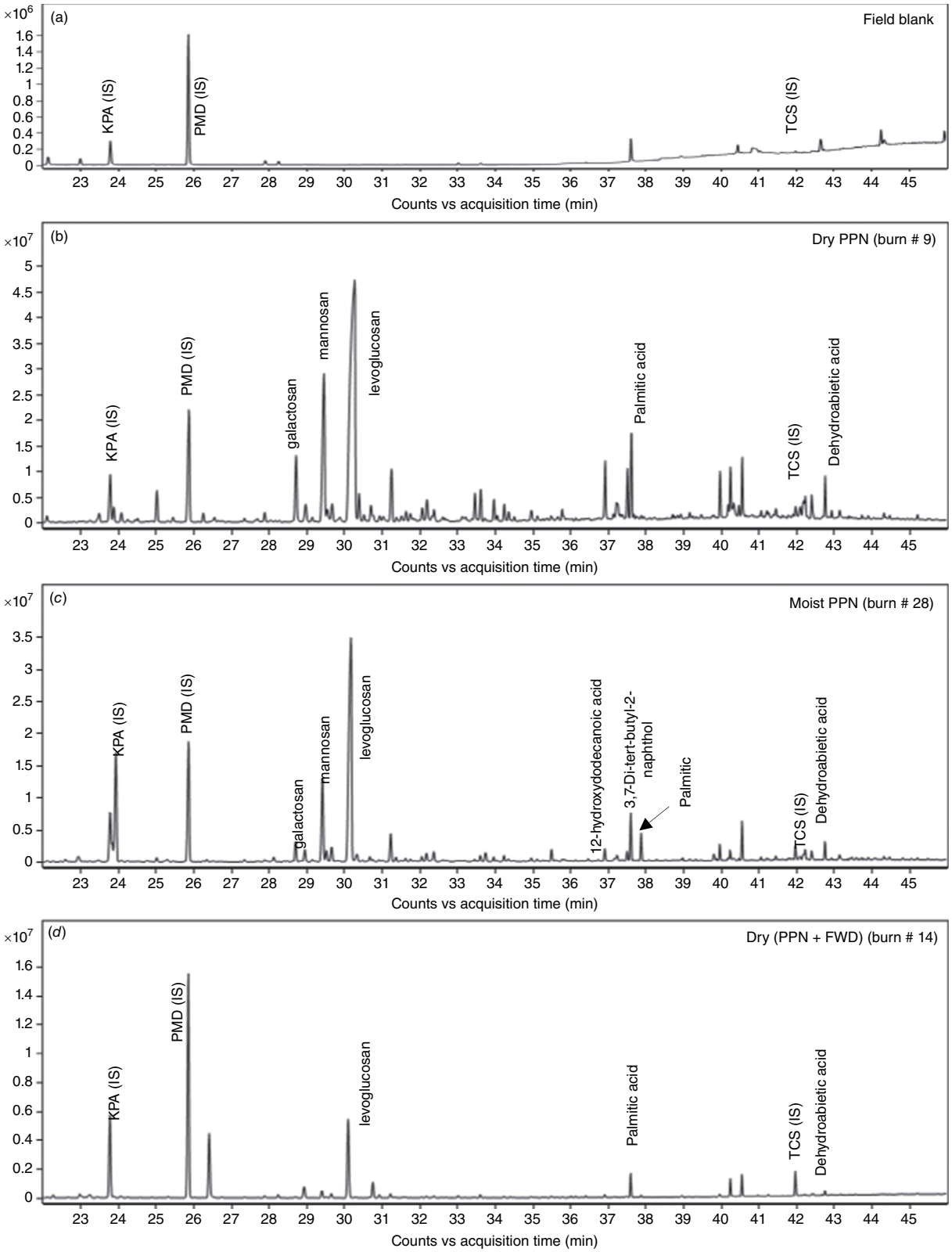

Fig. 2. Representative examples of GC-MS (portion 22–46 min) total ion chromatograms (TICs) associated with silylated smoke extracts (EI mode): (*a*) field blank; (*b*) dry PPN (burn #9); (*c*) moist PPN (burn #28); and (*d*) mixture of dry PPN and dry FWD (burn #14).

Table 2. Summary of selected oxygenated organic compounds identified in this study by GC-MS.

Nomenclature (formula)	Structure	Five abundant EI ions as TMS	MW (MW_{TMS}) (g mol^{-1})
Sugars and sugar alcohols			
Levoglucosan ($C_6H_{10}O_5$)	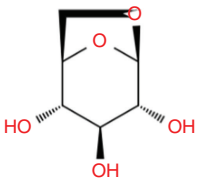	317, 289, 273, 363, 73	162 (378)
Mannosan ($C_6H_{10}O_5$)	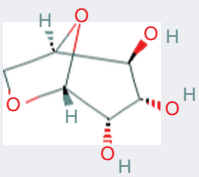	289, 273, 363, 199, 73	162 (378)
Galactosan ($C_6H_{10}O_5$)	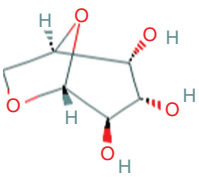	289, 273, 363, 199, 73	162 (378)
α-D-Glucopyranose ($C_6H_{12}O_6$)	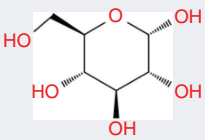	525, 451, 271, 361, 73	180 (540)
Xylose (two peaks) ($C_5H_{10}O_5$)	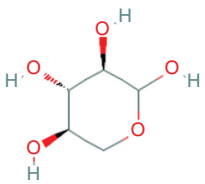	204, 217, 191, 73, 147	150 (438)
Inositol ($C_6H_{12}O_6$)	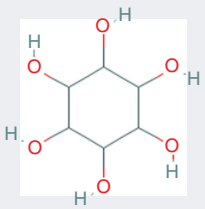	204, 217, 73, 147, 129	180 (612)
D-Arabitol ($C_5H_{12}O_5$)	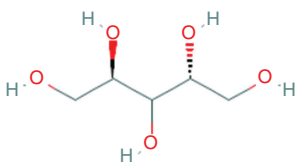	129, 243, 205, 317, 407	152 (512)
Mannitol ($C_6H_{14}O_6$)	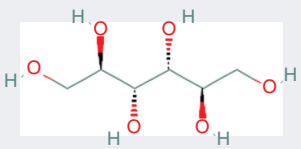	319, 73, 205, 217, 307	182 (614)

(*Continued on next page*)

Table 2. (*Continued*)

Nomenclature (formula)	Structure	Five abundant EI ions as TMS	MW (MW_{TMS}) (g mol^{-1})
Alkanoic acids			
n-Dodecanoic acid ($C_{12}H_{24}O_2$)	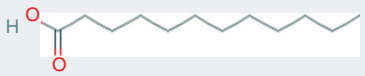	117, 73, 257, 132, 272	200 (272)
n-Hexadecanoic acid ($C_{16}H_{32}O_2$)	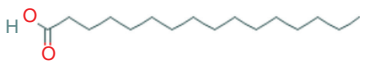	313, 117, 132,145, 73	256 (328)
12-Hydroxydodecanoic acid ($C_{12}H_{24}O_3$)		361, 345, 271, 389, 73	216 (360)
9,12-Octadecadienoic acid ($C_{18}H_{32}O_2$)		73, 75, 337, 262, 129	280 (352)
Diterpenoids			
Dehydroabietic acid ($C_{20}H_{28}O_2$)	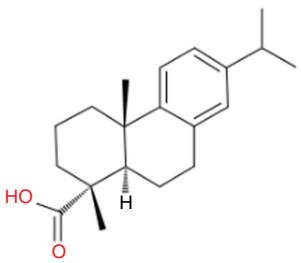	373, 357, 401, 255, 283	300 (372)
Communic acid ($C_{20}H_{30}O_2$)	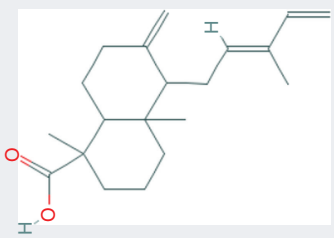	257, 375, 359, 403, 73	302 (374)
Abietic acid ($C_{20}H_{30}O_2$)	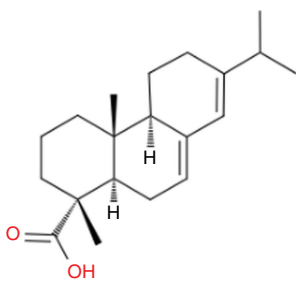	257, 375, 359, 403, 73	302 (374)
Pimaric acid ($C_{20}H_{30}O_2$)	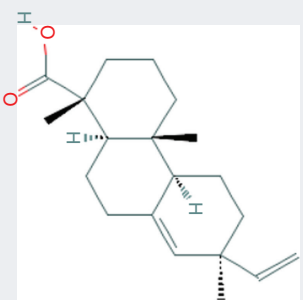	257, 375, 359, 403, 73	302 (374)

(*Continued on next page*)

Table 2. (*Continued*)

Nomenclature (formula)	Structure	Five abundant EI ions as TMS	MW (MW_{TMS}) (g mol^{-1})
Dihydroabietic acid ($C_{20}H_{32}O_2$)	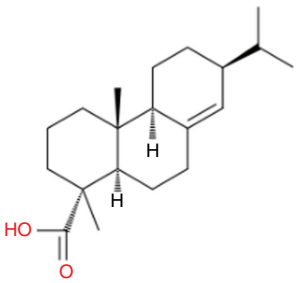	377, 361, 259, 405, 73	304 (376)
Isocupressic acid ($C_{20}H_{32}O_3$)	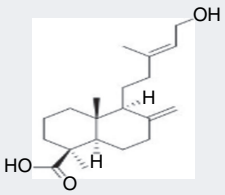	73, 359, 241, 256, 449	320 (464)
Imbricatoloic acid ($C_{20}H_{34}O_3$)	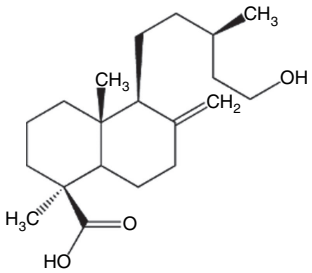	451, 467, 495, 507, 73	322 (466)
SVOCs/IVOCs			
Benzoic acid ($C_7H_6O_2$)	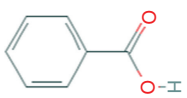	179, 195, 105, 73, 223	122 (194)
3-Hydroxybenzoic acid ($C_7H_6O_3$)	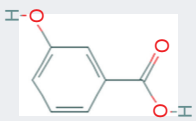	267, 283, 193, 73, 311	138 (282)
4-Hydroxybenzoic acid (three peaks) ($C_7H_6O_3$)	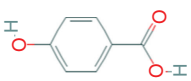	267, 283, 193, 73, 311	138 (282)
Benzeneethanol, 2-methoxy ($C_9H_{12}O_2$)	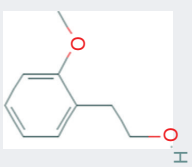	209, 73, 353, 225, 311	152 (224)
1,2-Benzenediol (three peaks) ($C_6H_6O_2$)	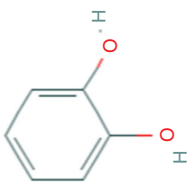	239, 255, 73, 283, 295	110 (254)

(*Continued on next page*)

Table 2. (*Continued*)

Nomenclature (formula)	Structure	Five abundant EI ions as TMS	MW (MW_{TMS}) (g mol^{-1})
2-Ethylphenol ($C_8H_{10}O$)	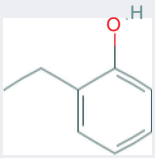	179, 195, 105, 73, 223	122 (194)
4-Ethylphenol ($C_8H_{10}O$)		179, 195, 105, 73, 223	122 (194)
Vanillic acid ($C_8H_8O_4$)	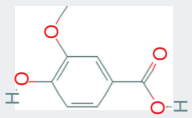	297, 313, 223, 341, 73	168 (312)
Phthalic acid ($C_8H_6O_4$)	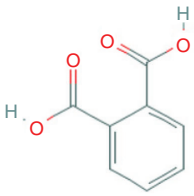	147, 73, 295, 221, 310	166 (310)
Isophthalic acid ($C_8H_6O_4$)	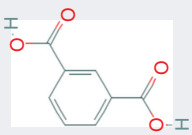	295, 279, 310, 205, 177	166 (310)
Syringic acid (two peaks) ($C_9H_{10}O_5$)	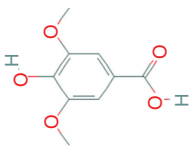	327, 343, 239, 73, 383	198 (342)
4-Methylcatecol ($C_7H_8O_2$)	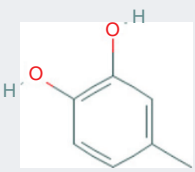	253, 269, 297, 123, 186	124 (268)
3-Methylcatecol ($C_7H_8O_2$)	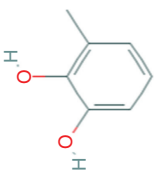	253, 269, 297, 123, 186	124 (268)
1,2,3-Benzenetriol ($C_6H_6O_3$)	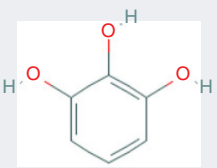	327, 343, 73, 371, 73	126 (342)
Homovanillic acid ($C_9H_{10}O_4$)	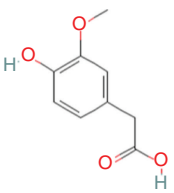		182 (326)

(*Continued on next page*)

Table 2. (*Continued*)

Nomenclature (formula)	Structure	Five abundant EI ions as TMS	MW (MW_{TMS}) ($g\ mol^{-1}$)
Sinapyl alcohol ($C_{11}H_{14}O_4$)	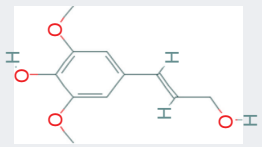	355, 339, 265, 383, 73	210 (354)
p-Coumaric acid ($C_9H_8O_3$)	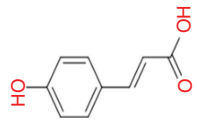	309, 293, 337, 109, 73	164 (308)
p-Coumaryl alcohol ($C_9H_{10}O_2$)	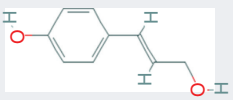	279, 295, 323, 335, 73	150 (294)
Sinapinic acid ($C_{11}H_{12}O_5$)	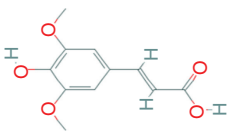	279, 353, 369, 397, 409	224 (368)
Caffeyl alcohol ($C_9H_{10}O_3$)	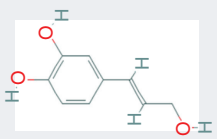	383, 267, 411, 293, 257	166 (382)
Coniferyl alcohol (four isomers) ($C_{10}H_{12}O_3$)	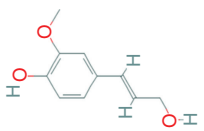	325, 309, 235, 217, 353	180 (324)
4,4′- Methylenebisphenol ($C_{13}H_{12}O_2$)	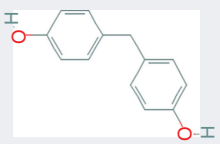	345, 329, 373, 255, 385	200 (344)
3,7-Di-*tert*-butyl-2-naphthol (two peaks) ($C_{18}H_{24}O$)	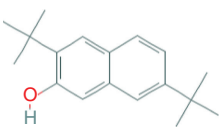	327, 329, 313, 357, 369	256 (328)
Dihydro-5-(hydroxymethyl)-2(3*H*)-furanone ($C_5H_8O_3$)	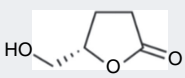	99, 173, 189, 217, 229	116 (188)

PPN only. Additional identified sugars and sugar alcohols include α-D-glucopyranose, xylose, inositol, arabitol, and mannitol (Table 2). The presence in PPN aerosol of sugar alcohols (e.g. arabitol and manitol), used in the literature as fungal spore tracers (e.g. Xu *et al.* 2019), suggests that PPN contribute also to these sugar alcohols in an area dominated by pine trees.

n-alkanes/fatty acids/alcohols

$PM_{2.5}$ generated in this study is dominated by oxygenated ring-retaining compounds. However, several oxygenated compounds with linear structure were identified in this study including mid-chain *n*-alkanes: dodecanoic acid, palmitic acid, 12-hydroxydodecanoic acid, and 9,12-octadecadienoic acid (Table 2). These compounds have been identified based on authentic standards. The CI mass spectrum of the BSTFA derivative of palmitic acid shows fragment ions at *m/z* 73, 239 [$M^{+\cdot}$ – 89], 313 [$M^{+\cdot}$ – 15], and 327 [$M^{+\cdot}$ – 1]; and adducts at 328 [$M^{+\cdot}$ + 1], 357 [$M^{+\cdot}$ + 29], 369 [$M^{+\cdot}$ + 41], and 401 [$M^{+\cdot}$ + 73]. These fragments and the adducts are consistent with the presence of one –OH group and a MW of 328 for the derivatised compound and 256 for the underivatised compound. Several small peaks eluting between 40.8 and 42.8 min could not be identified, however, their

mass spectra are consistent with long-chain alkanes (fatty acids and alcohols with a carbon number between C18 and C35). Recently, fatty acids and alcohols, mainly C27 and C29, have been reported in atmospheric aerosol and in pine needle extracts (Kim *et al.* 2017; Miyazaki *et al.* 2019; Nikolić *et al.* 2020; Liang *et al.* 2021). High abundances of *n*-alkanes have been measured in ambient $PM_{2.5}$ collected all over the world (e.g., Kang *et al.* 2018 and reference therein). A wide variety of sources including plant waxes (Kawamura *et al.* 2003), anthropogenic activity (e.g. fossil fuel use) (Kang *et al.* 2016), and biomass burning (Schauer *et al.* 2001) were reported to contribute to their emission. While these species have been reported previously in several studies, their detection for the first time in PPN aerosol in this study provides evidence that PPN contribute to their emission in an area dominated by ponderosa pine trees.

Diterpenoids

Many relatively smaller peaks were observed to elute late in the chromatograms (Fig. 2), reflecting the complexity of smoke particles that originated during PPN combustion. In this study, several diterpenoids were identified and associated with some of these peaks including dehydroabietic acid, communic acid, abietic acid, pimaric acid, dihydroabietic acid, isocupressic acid, and imbricatoloic acid (Table 2). Supplementary Fig. S1 displays CI and EI mass spectra associated with isocupressic acid-2TMS, dihydroabietic acid-1TMS, and imbricatoloic-1TMS. For example, the CI mass spectrum of the TMS derivative of isocupressic acid (Supplementary Fig. S1, top) shows fragment ions at *m/z* 73, 133, 191, 207, 265, 309, 343, 359 [$M^{+\cdot}$ – 105], 375 [$M^{+\cdot}$ – 89], 433, and 449 [$M^{+\cdot}$ – 15] and adducts at *m/z* 465 [$M^{+\cdot}$ + 1], 507 [$M^{+\cdot}$ + 41], and 539 [$M^{+\cdot}$ + 75]. These fragments and adducts are consistent with the presence of two –OH groups and a MW of 464 for the derivatised compound and a MW of 320 for the underivatised compound. The presence of a peak at *m/z* 305 [$M^{+\cdot}$ – 105] is consistent with a compound bearing an alcoholic –OH group. The fragments ions observed in EI mode in Supplementary Fig. S1*b* are consistent with isocupressic acid-2TMS. Similar analysis of the remaining EI and CI mass spectra shown in Supplementary Fig. S1 are consistent with dehydroabietic acid and imbricatoloic acid. Oxygenated diterpenoids are well documented in the literature and have been identified in a wide range of plant extracts including pine needles and twigs (e.g. Gardner *et al.* 1999). Diterpenoids are used as markers in biomass burning emissions for conifer combustion (Hays *et al.* 2002; Liang *et al.* 2021). Recently, selected diterpenoids were identified in atmospheric aerosol samples collected during the 2017 Northern California wildfires (Liang *et al.* 2021). In line with our finding in this study, pine tree needles which are widely distributed in Northern California could be a potential source of diterpenoids as observed by Liang *et al.* (2021). Dehydroabietic acid was reported to thermally decompose in fires to form 7-oxo-dehydroabietic acid (proposed as an aging product of resin acids: Yan *et al.* 2008) and retene (Ramdahl 1983; Simoneit *et al.* 1993; Standley and Simoneit 1994), however, in a recent study by Liang *et al.* (2021), 7-oxo-dehydroabietic acid was suggested to be a useful indicator for the formation of biomass burning SOA. In our study, neither 7-oxo-dehydroabietic acid or retene were detected, therefore it is likely that the chemicals reported in this study are of primary origin. The emissions of a wide range of diterpenoids observed in this study are likely due to the distillation from unburned heated PPN.

Intermediate-volatile and semi-volatile organic compounds (IVOCs/SVOCs)

Other ring-retaining compounds with one or more –OH and –COOH groups were identified in this study (Table 2). They are classified either as IVOCs or SVOCs (Shen *et al.* 2023 and reference therein) based on their volatility, and include benzoic acid, 3-hydroxybenzoic acid, 4-hydroxybenzoic acid (and two additional isomers), 2-methoxybenzene ethanol, catechol (and two additional isomers), 2-ethylphenol, 4-ethylphenol, vanillic acid, syringic acid (and one additional isomer), 4-methylcatechol, and 1,2,3-benzenetriol. Other IVOCS and SVOCs containing one benzene ring and one external double bond were also identified, including sinapyl alcohol, *p*-coumaric acid, *p*-coumaryl alcohol, sinapinic acid, caffeyl alcohol, and coniferyl alcohol. The majority of SVOCs and IVOCs (Table 2) were identified based on authentic standards. Additional small peaks were detected in chromatograms in Fig. 2, for which their associated mass spectra are consistent with SVOCs and IVOCs, however, their structure and formulae could not be obtained based on the analytical method used in this study. Many IVOCs and SVOCs identified here have been reported to be emitted directly from biomass fires in the gas phase (Grieshop *et al.* 2009*a*, 2009*b*; May *et al.* 2013; Hatch *et al.* 2018). Their detection in the particle phase in this study suggests their gas-phase partitioning or their direct emission as primary volatile organic compounds into the particle phase. In the literature, some of these IVOCs and SVOCs have been reported in part to be the result of photochemical and/or aging processes of primary emitted VOCs (Liang *et al.* 2021; Li *et al.* 2023). However, in our chamber, photochemistry could not occur due to the absence of sunlight. Some of these compounds may also undergo gas-phase reactions and participate in SOA formation and then partition to the particle phase (Donahue *et al.* 2013; May *et al.* 2013; Alvarado *et al.* 2015). The extent of pollutant formation from wildfire emissions is dependent in part on the speciation of SVOCs and IVOCs.

Effect of fuel type and moisture on the composition of $PM_{2.5}$ smoke

The chromatograms in Fig. 2 can be directly compared because the sampling time and flow rate of each burn were the same. A detailed examination of mass spectra

associated with each peak detected in these chromatograms revealed significant changes in the composition of particles depending on the amount and type of fuel burned (e.g., dry vs moist PPN; dry PPN vs mixture of dry PPN + FWD). The main peaks were detected in all chromatograms (Fig. 2) except in the blank, although at variable abundance. The addition of FWD to moist PPN, or dry PPN, as illustrated in burn #14, resulted in a substantial decrease in the number and intensity of peaks detected (Fig. 2). This is clearly illustrated by the filter colours from burns #9, #28, and #14, respectively (Fig. 3), indicating distinct differences in the compounds formed from the different fuels burned. Similar results were reported for the formation of SOA from the oxidation of isoprene as a function of relative humidity (Nestorowicz *et al.* 2018). The burn integrated MCEs, as described previously (Urbanski 2013), ranged from 0.91 to 0.97 (Table 3; Landis *et al.* 2021) representing a range of predominantly flaming combustion conditions (Akagi *et al.* 2011, 2013). This is consistent with the formation of black carbon (Fig. 4), which is formed under flaming conditions rather than smouldering conditions (Garg *et al.* 2021 and reference therein). Due to soot particles collected on filters, Fig. 4 bottom also shows photographs of the corresponding filter extracts, which clearly displays a yellow hue, particularly for E1 and E2, that is close in appearance to filters previously collected in this laboratory from toluene/NOx experiments (Jaoui *et al.* 2008). A systematic analysis of mass spectra associated with peaks recorded in this study, using the analysis reported by Jaoui *et al.* (2018), revealed the presence of oxygenated compounds bearing nitro groups (NACs). Therefore, the yellow colour is probably associated either with the presence of aromatic ring, nitrogen containing compounds, and/or ketone/aldehyde groups (Table 2) (Jaoui *et al.* 2008; Garg *et al.* 2021). Filter/extract F4/E4 has lost most of the colour of F1/E1 and F2/E2, which is consistent with the significant decrease in peaks detected, primarily those associated with compounds containing an aromatic ring (peaks eluted between 31 and 36 min: Fig. 2). The addition of FWD to the PPN produced material (filter F4/E4) of a deep dark colour, likely due to soot particles formed from FWD. Finally, the particles from the dry + moist PPN resulted in filter F2 having a pronounced yellow colour, although considerably lighter than that from the moist or dry PPN alone. The filters and extracts pictures were taken from the same camera, and all conditions for taking images such as light and position are the same.

Although a detailed qualitative analysis was performed in this study, the concentrations of a subset of compounds of interest, which were also found in ambient aerosol (Liang *et al.* 2021, 2022), were quantified to investigate the chemical changes at the molecular level in going from dry PPN (base case) to the other mixtures shown in Fig. 2. Table 3 presents the estimated concentrations of methylcatechol, levoglucosan, mannosan, galactosan, D-arabitol, palmitic acid, dehydroabietic acid, and isocupressic acid. The quantification was performed using a single derivatisation with BSTFA that was evaluated previously (Jaoui *et al.* 2004, 2006). For each compound, the extracted ion chromatogram of the most intensive ions was used for quantification, depending on the degree of coelution. Using our best estimate of the calibration factors, concentrations for each of the target compounds for $PM_{2.5}$ samples were determined and are provided in Table 3. Table 3 also includes the measured $PM_{2.5}$ concentration and MCE (Landis *et al.* 2021) and the initial fuel mass used in each experiment. Authentic standards or surrogates for those that are not available commercially were used for quantification/semi-quantification. The chamber samples were GC-MS analysed prior to receiving some authentic standards; therefore, no authentic standards were used in this study for these products.

The changes in moisture content (burn #9 versus burn #28) resulted in the product concentrations (normalised to $PM_{2.5}$) in the moist PPN burn decreasing significantly (59% decrease in levoglucosan, 68% decrease in palmitic acid, and 65% decrease in dehydroabietic acid). It is likely that the production of OOCs is partially suppressed in the presence of water in the system. Burning a mixture of dry PPN and FWD alone also resulted in a pronounced decrease in the concentration of these products compared either to dry PPN or moist PPN. This decrease may have resulted from a lower combustion temperature (not measured in this study) when a mixture of PPN and FWD is burned. The concentrations of levoglucosan, mannosan, and galactosan were found to decrease as the combustion temperature increased (Kuo *et al.* 2011).

Conclusions

In the present study, laboratory experiments were conducted to investigate the chemical composition at the molecular level of $PM_{2.5}$ that originated from the combustion of mixed dry and moist ponderosa pine needles and in the presence and absence of ponderosa pine fine woody debris. Chamber $PM_{2.5}$ collected under these conditions has been analysed for oxygenated organic compounds bearing –OH and –COOH groups using derivatisation methods followed by gas chromatography–mass spectrometry. While a detailed non-targeted analysis has been made, our primary focus has been to examine the class of compounds that may be present in ambient aerosol affected by wildfires.

More than 50 oxygenated organic compounds bearing –OH and/or –COOH groups were identified. Four classes of compounds including (1) sugars and sugar alcohols, (2) *n*-alkanes/fatty acids and alcohols, (3) diterpenoids, and (4) I/SVOCs were found in each of the systems studied, albeit at various concentrations. The major products were levoglucosan and mannosan (sugars); *n*-dodecanoic acid and *n*-hexadecanoic acid (alkanes); dihydroabietic

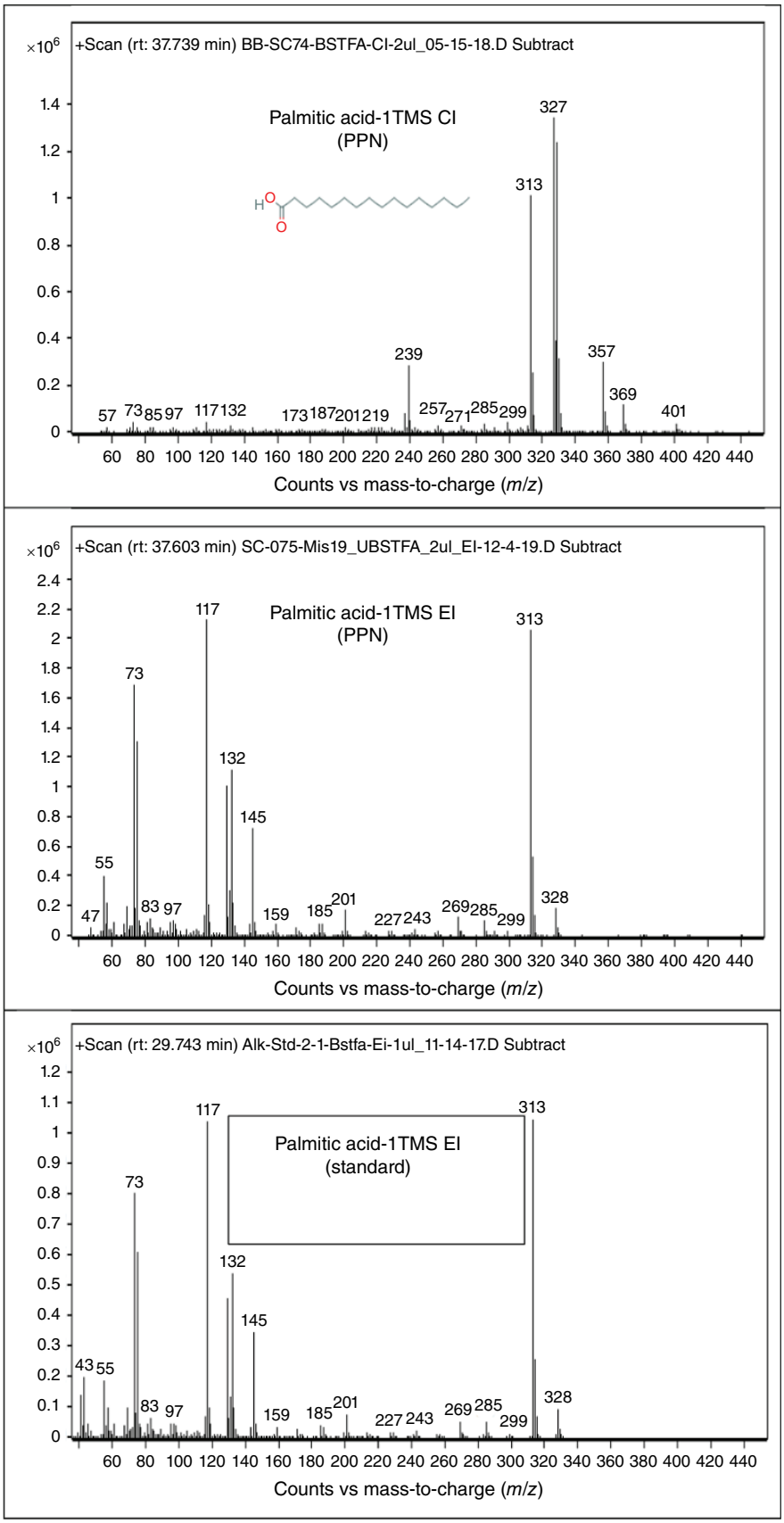

Fig. 3. Mass spectra of TMS derivatives recorded in methane-CI and EI (70 eV) of palmitic acid observed in smoke particles ($PM_{2.5}$) collected during pine needle combustion.

Table 3. MCE and concentrations of $PM_{2.5}$ and selected products identified in three experiments conducted in this study.

Type	PPN dry (base) case)	PPN moist	PPN + FWD
Burn	#9	#28	#14
MCE	0.957	0.946	0.967
$PM_{2.5}$ ($\mu g\,m^{-3}$)	1814.9	541.9	715.6
Methylcatechol (Mct)			
Conc. Mct ($\mu g\,m^{-3}$)*	0.49	0	0.02
[Mct]/[$PM_{2.5}$] ratio	0.00030	0	0.00003
Percentage change	–	−100	−95
Levoglucosan (LG)			
Conc. LG ($\mu g\,m^{-3}$)**	25.9	10.6	1.44
[LG]/[$PM_{2.5}$] ratio	0.0143	0.0196	0.0014
Percentage change	–	−100	−95
Mannosan (Mn)			
Conc. Mn ($\mu g\,m^{-3}$)**	8.35	2.96	0.10
[Mn]/[$PM_{2.5}$] ratio	0.0046	0.0055	0.001
Percentage change	–	−65	−99
Galactosan (Gts)			
Conc. Gts ($\mu g\,m^{-3}$)**	1.40	0.30	0
[Gts]/[$PM_{2.5}$] ratio	0.0008	0.0005	0
Percentage change	–	−65	−99
D-Arabitol (Ar)			
Conc. Ar ($\mu g\,m^{-3}$)***	0.47	0.02	0.02
[Ar]/[$PM_{2.5}$] ratio	0.0003	0.00003	0.00002
Percentage change	–	−96	−97
Palmitic acid (PtA)			
Conc. PtA ($\mu g\,m^{-3}$)***	2.18	0.69	0.17
[PtA]/[$PM_{2.5}$] ratio	0.0012	0.0013	0.0002
Percentage change	–	−68	−92
Dehydroabietic acid (DHAA)			
Conc DHAA ($\mu g\,m^{-3}$)*	2.47	0.86	0.09
[DHAA]/[$PM_{2.5}$] ratio	0.0014	0.0016	0.00001
Percentage change	–	−65	−96
Isocupressic acid (ICA)			
Conc. ICA ($\mu g\,m^{-3}$)*	0.09	0.03	0.002
[ICA]/[$PM_{2.5}$] ratio	0.00051	0.000061	0.000002
Percentage change	–	−64	−98

The percentage change values given in columns 3 and 4 are for going from dry PPN to moist PPN (column 3), and from dry PPN to dry PPN + FWD (column 4). Phthalic acid (*), levoglucosan (**), and D-arabic acid (***) were used for quantification purposes.

acid, isocupressic acid, and dehydroabietic acid (diterpenes), and a series of IVOCs and SVOCs. The presence of some of these products (IVOCs/SVOCS) in the gas and particle phases provides evidence of their gas/particle partitioning. Most compounds detected in ponderosa pine needle particles have unknown health impacts and were also reported to form in ambient particles. The present study highlights the potential of PPN constituents and their importance and contribution to

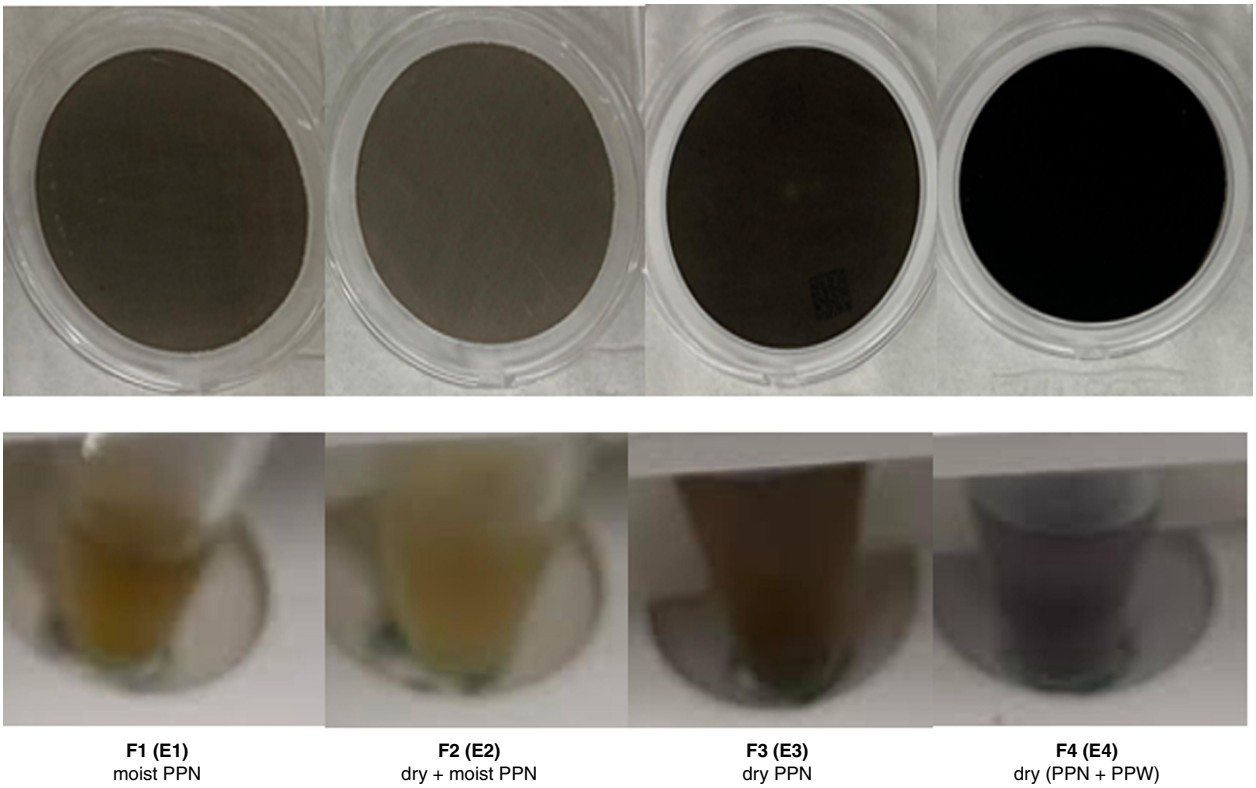

Fig. 4. Effect of fuel changes in filter (F: top) and extract (E: bottom) appearance in going from the moist PPN filter (F1) to subsequent mixtures. Note: the same volume of air was sampled on each filter.

ambient aerosol generated during forest fires dominated by pine trees. For example, SVOCs were reported to evaporate from the particle phase in smoke plumes when transported downwind, and they may react with atmospheric oxidants leading to O_3 and SOA formation (Liang *et al.* 2022). Therefore, with better speciation of compounds in wildfires and an understanding of their sources and contribution to ambient aerosol, more targeted toxicological studies could be carried out to elucidate their health impacts. Furthermore, the results of this study can contribute to more accurate exposure assessments from wildfire smoke in general. Sugars (levoglucosan and mannosan) and diterpenoids were observed in ambient samples in areas impacted by wildfires. In addition to their diverse sources, the combustion of pine needles as a source is demonstrated in this paper. This study also examines the effect of fuel moisture content level on $PM_{2.5}$ and its oxygenated components.

Supplementary material

Supplementary material is available online.

References

Akagi SK, Yokelson RJ, Wiedinmyer C, Alvarado MJ, Reid JS, Karl T, Crounse JD, Wennberg PO (2011) Emission factors for open and domestic biomass burning for use in atmospheric models. *Atmospheric Chemistry and Physics* **11**, 4039–4072. doi:10.5194/acp-11-4039-2011

Akagi SK, Yokelson RJ, Burling IR, Meinardi S, Simpson I, Blake DR, McMeeking GR, Sullivan A, Lee T, Kreidenweis S, Urbanski S, Reardon J, Griffith DWT, Johnson TJ, Weise DR (2013) Measurements of reactive trace gases and variable O_3 formation rates in some South Carolina biomass burning plumes. *Atmospheric Chemistry and Physics* **13**, 1141–1165. doi:10.5194/acp-13-1141-2013

Alvarado MJ, Lonsdale CR, Yokelson RJ, Akagi SK, Coe H, Craven JS, Fischer EV, McMeeking GR, Seinfeld JH, Soni T, Taylor JW, Weise DR, Wold CE (2015) Investigating the links between ozone and organic aerosol chemistry in a biomass burning plume from a prescribed fire in California chaparral. *Atmospheric Chemistry and Physics* **15**, 6667–6688. doi:10.5194/acp-15-6667-2015

Balch JK, Bradley BA, Abatzoglou JT, Nagy RC, Fusco EJ, Mahood AL (2017) Human-started wildfires expand the fire niche across the United States. *Proceedings of the National Academy of Sciences of the United States of America* **114**, 2946–2951. doi:10.1073/pnas.1617394114

Bankova V, Bertelli D, Borba R, Conti BJ, da Silva Cunha IB, Danert C, Eberlin MN, I Falcão S, Isla MI, Moreno MIN, Papotti G, Popova M, Santiago KB, Salas A, Sawaya ACHF, Schwab NV, Sforcin JM, Simone-Finstrom M, Spivak M, Trusheva B, Vilas-Boas M, Wilson M, Zampini C (2019) Standard methods for *Apis mellifera* propolis research. *Journal of Apicultural Research* **58**(2), 1–49. doi:10.1080/00218839.2016.1222661

Baylon P, Jaffe DA, Wigder NL, Gao H, Hee J (2015) Ozone enhancement in western US wildfire plumes at the Mt. Bachelor Observatory: the role of NO_x. *Atmospheric Environment* **109**, 297–304. doi:10.1016/j.atmosenv.2014.09.013

Bladon KD, Emelko MB, Silins U, Stone M (2014) Wildfire and the Future of Water Supply. *Environmental Science & Technology* **48**(16), 8936–8943. doi:10.1021/es500130g

Bond TC, Streets DG, Yarber KF, Nelson SM, Woo JH, Klimont Z (2004) A technology-based global inventory of black and organic carbon

emissions from combustion. *Journal of Geophysical Research* **109**, D14203. doi:10.1029/2003JD003697

Bowman DMJS, Balch JK, Artaxo P, Bond WJ, Carlson JM, Cochrane MA, D'Antonio CM, Defries RS, Doyle JC, Harrison SP, Johnston FH, Keeley JE, Krawchuk MA, Kull CA, Marston JB, Moritz MA, Prentice IC, Roos CI, Scott AC, Swetnam TW, van der Werf GR, Pyne SJ (2009) Fire in the Earth system. *Science* **324**, 481–484. doi:10.1126/science.1163886

Bowman DMJS, Balch J, Artaxo P, Bond WJ, Cochrane MA, D'Antonio CM, DeFries R, Johnston FH, Keeley JE, Krawchuk MA, Kull CA, Mack M, Moritz MA, Pyne S, Roos CI, Scott AC, Sodhi NS, Swetnam TW, Whittaker R (2011) The human dimension of fire regimes on Earth. *Journal of Biogeography* **38**(12), 2223–2236. doi:10.1111/j.1365-2699.2011.02595.x

Briggs NL, Jaffe DA, Gao H, Hee JR, Baylon PM, Zhang Q, Zhou S, Collier SC, Sampson PD, Cary RA (2016) Particulate matter, ozone, and nitrogen species in aged Wildfire plumes observed at the Mount Bachelor observatory. *Aerosol and Air Quality Research* **16**, 3075–3087. doi:10.4209/aaqr.2016.03.0120

Burke M, Driscoll A, Heft-Neal S, Xue J, Burney J, Wara M (2021) The changing risk and burden of wildfire in the United States. *Proceedings of the National Academy of Sciences* **118**(2), doi:10.1073/pnas.2011048118

Cheng Y, Engling G, He KB, Duan FK, Ma YL, Du ZY, Liu JM, Zheng M, Weber RJ (2013) Biomass burning contribution to Beijing aerosol. *Atmospheric Chemistry and Physics* **13**, 7765–7781. doi:10.5194/acp-13-7765-2013

Christian TJ, Kleiss B, Yokelson RJ, Holzinger R, Crutzen PJ, Hao WM, Shirai T, Blake DR (2004) Comprehensive laboratory measurements of biomass-burning emissions: 2. First intercomparison of open-path FTIR, PTR-MS, and GC- MS/FID/ECD. *Journal of Geophysical Research* **109**, D02311. doi:10.1029/2003JD003874

Crutzen PJ, Andreae MO (1990) Biomass burning in the tropics: impact on atmospheric chemistry and biogeochemical cycles. *Science* **250**(4988), 1669–1678. doi:10.1126/science.250.4988.1669

Decesari S, Fuzzi S, Facchini MC, Mircea M, Emblico L, Cavalli F, Maenhaut W, Chi X, Schkolnik G, Falkovich A, Rudich Y, Claeys M, Pashynska V, Vas G, Kourtchev I, Vermeylen R, Hoffer A, Andreae MO, Tagliavini E, Moretti F, Artaxo P (2006) Characterization of the organic composition of aerosols from Rondônia, Brazil, during the LBA-SMOCC 2002 experiment and its representation through model compounds. *Atmospheric Chemistry and Physics* **6**, 375–402. doi:10.5194/acp-6-375-2006

Donahue NM, Chuang W, Epstein SA, Kroll JH, Worsnop DR, Robinson AL, Adams PJ, Pandis SN (2013) Why do organic aerosols exist? Understanding aerosol lifetimes using the two-dimensional volatility basis set. *Environmental Chemistry* **10**, 151–157. doi:10.1071/EN13022

Gardner DR, Panter KE, James LF (1999) Pine needle abortion in cattle: metabolism of isocupressic acid. *Journal of Agricultural and Food Chemistry* **47**(7), 2891–2897. doi:10.1021/jf981322d

Garg P, Roche T, Eden M, Matz J, Oakes JM, Bellini C, Gollner MJ (2021) Effect of moisture content and fuel type on emissions from vegetation using a steady state combustion apparatus. *International Journal of Wildland Fire* **30**, 14–23. doi:10.1071/WF20118

Gonçalves C, Alves C, Fernandes AP, Monteiro C, Tarelho L, Evtyugina M, Pio C (2011) Organic compounds in $PM_{2.5}$ emitted from fireplace and woodstove combustion of typical Portuguese wood species. *Atmospheric Environment* **45**, 4533–4545. doi:10.1016/j.atmosenv.2011.05.071

Grieshop AP, Miracolo MA, Donahue NM, Robinson AL (2009*a*) Constraining the volatility distribution and gas-particle partitioning of combustion aerosols using isothermal dilution and thermodenuder measurements. *Environmental Science and Technology* **43**, 4750–4756. doi:10.1021/es8032378

Grieshop AP, Logue JM, Donahue NM, Robinson AL (2009*b*) Laboratory investigation of photochemical oxidation of organic aerosol from wood fires 1: measurement and simulation of organic aerosol evolution. *Atmospheric Chemistry and Physics* **9**, 1263–1277. doi:10.5194/acp-9-1263-2009

Guenther A (2002) The contribution of reactive carbon emissions from vegetation to the carbon balance of terrestrial ecosystems. *Chemosphere* **49**(8), 837–844. doi:10.1016/s0045-6535(02)00384-3

Hatch LE, Luo W, Pankow JF, Yokelson RJ, Stockwell CE, Barsanti KC (2015) Identification and quantification of gaseous organic compounds emitted from biomass burning using two-dimensional gas chromatography–time-of-flight mass spectrometry. *Atmospheric Chemistry and Physics* **15**, 1865–1899. doi:10.5194/acp-15-1865-2015

Hatch LE, Rivas-Ubach A, Jen CN, Lipton M, Goldstein AH, Barsanti KC (2018) Measurements of I/SVOCs in biomass-burning smoke using solid-phase extraction disks and two-dimensional gas chromatography. *Atmospheric Chemistry and Physics* **18**, 17801–17817. doi:10.5194/acp-18-17801-2018

Hays MD, Geron CD, Linna KJ, Smith ND, Schauer JJ (2002) Speciation of gas-phase and fine particle emissions from burning of foliar fuels. *Environmental Science and Technology* **36**, 2281–2295. doi:10.1021/es0111683

Holden ZA, Swanson A, Luce CH, Jolly WM, Maneta M, Oyler JW, Warren DA, Parsons R, Affleck D (2018) Decreasing fire season precipitation increased recent western US forest wildfire activity. *Proceedings of the National Academy of Sciences of the United States of America* **115**(36), E8349–E8357. doi:10.1073/pnas.1802316115

Hosseini S, Urbanski P, Qi D, Burling IR, Yokelson R,J, Johnson TJ, Shrivastava M, Jung HS, Weise DR, Miller JW, Cocker III DR (2013) Laboratory characterization of PM emissions from combustion of wildland biomass fuels. *Journal of Geophysical Research: Atmospheres* **118**, 9914–9929. doi:10.1002/jgrd.50481

Hou S, Liu D, Xu J, Vu TV, Wu X, Srivastava D, Fu P, Li L, Sun Y, Vlachou A, Moschos V, Salazar G, Szidat S, Prévôt ASH, Harrison RM, Shi Z (2021) Source apportionment of carbonaceous aerosols in Beijing with radiocarbon and organic tracers: insight into the differences between urban and rural sites. *Atmospheric Chemistry and Physics* **21**, 8273–8292. doi:10.5194/acp-21-8273-2021

Jaoui M, Kleindienst TE, Lewandowski M, Edney EO (2004) Identification and quantification of aerosol polar oxygenated compounds bearing carboxylic or hydroxyl groups. 1. Method development. *Analytical Chemistry* **76**, 4765–4778. doi:10.1021/ac049919h

Jaoui M, Kleindienst TE, Lewandowski M, Offenberg JH, Edney EO (2005) Identification and quantification of aerosol polar oxygenated compounds bearing carboxylic or hydroxyl groups. 2. Organic tracer compounds from monoterpenes. *Environmental Science and Technology* **39**, 5661–5673. doi:10.1021/es048111b

Jaoui M, Corse E, Kleindienst TE, Offenberg JH, Lewandowski M, Edney EO (2006) Analysis of secondary organic aerosol compounds from the photooxidation of *d*-limonene in the presence of NO_X and their detection in ambient $PM_{2.5}$. *Environmental Science & Technology* **40**(12), 3819–3828. doi:10.1021/es052566z

Jaoui M, Edney EO, Kleindienst TE, Lewandowski M, Offenberg JH, Surratt JD, Seinfeld JH (2008) Formation of secondary organic aerosol from irradiated α-pinene/toluene/NO_x mixtures and the effect of isoprene and sulfur dioxide. *Journal of Geophysical Research* **113**, D09303. doi:10.1029/2007JD009426

Jaoui M, Lewandowski M, Offenberg JH, Colon M, Docherty KS, Kleindienst TE (2018) Characterization of aerosol nitroaromatic compounds: validation of an experimental method. *Journal of Mass Spectrometry* **53**, 680–692. doi:10.1002/jms.4199

Jen CN, Hatch LE, Selimovic V, Yokelson RJ, Weber R, Fernandez AE, Kreisberg NM, Barsanti KC, Goldstein AH (2019) Speciated and total emission factors of particulate organics from burning western US wildland fuels and their dependence on combustion efficiency. *Atmospheric Chemistry and Physics* **19**, 1013–1026. doi:10.5194/acp-19-1013-2019

Jolleys MD, Coe H, McFiggans G, Capes G, Allan JD, Crosier J, Williams PI, Allen G, Bower KN, Jimenez JL, Russell LM, Grutter M, Baumgardner D (2012) Characterizing the aging of biomass burning organic aerosol by use of mixing ratios: a meta-analysis of four regions. *Environmental Science and Technology* **46**(24), 13,093–13,102. doi:10.1021/es302386v

Jolleys MD, Coe H, McFiggans G, McMeeking GR, Lee T, Kreidenweis SM, Collett Jr JL, Sullivan AP (2014) Organic aerosol emission ratios from the laboratory combustion of biomass fuels. *Journal of Geophysical Research: Atmospheres* **119**, 12,850–12,871. doi:10.1002/2014JD021589

Kang M, Fu P, Aggarwal SG, Kumar S, Zhao Y, Sun Y, Wang Z (2016) Size distributions of *n*-alkanes, fatty acids and fatty alcohols in springtime

aerosols from New Delhi, India. *Environmental Pollution* **219**, 957–966. doi:10.1016/j.envpol.2016.09.077

Kang M, Ren L, Ren H, Zhao Y, Kawamura K, Zhang H, Wei L, Sun Y, Wang Z, Fu P (2018) Primary biogenic and anthropogenic sources of organic aerosols in Beijing, China: insights from saccharides and *n*-alkanes. *Environmental Pollution* **243**, 1579–1587. doi:10.1016/j.envpol.2018.09.118

Kawamura K, Ishimura Y, Yamazaki K (2003) Four years' observations of terrestrial lipid class compounds in marine aerosols from the western North Pacific. *Global Biogeochemical Cycles* **17**(1), 1003. doi:10.1029/2001GB001810

Kim SJ, Park SY, Lee J, Chang M, Chung Y, Lee T-K (2017) Biochemical compositions and biological activities of extracts from 3 species of Korean pine needles. *Journal of Food and Nutrition Research* **5**(1), 31–36. doi:10.12691/jfnr-5-1-6

Kononenko I (2017) Molecular characterization and ageing of the sandarac resin and its principal component communic acid. PhD Thesis, UPMC, Sorbonne University, Paris, France.

Krug J, Long R, Colón M, Habel A, Urbanski S, Landis MS (2021) Evaluation of small form factor, filter-based $PM_{2.5}$ samplers for temporary non-regulatory monitoring during wildland fire smoke events. *Atmospheric Environment* **265**, 118718. doi:10.1016/j.atmosenv.2021.118718

Kundu S, Kawamura K, Andreae TW, Hoffer A, Andreae MO (2010) Diurnal variation in the water-soluble inorganic ions, organic carbon and isotopic compositions of total carbon and nitrogen in biomass burning aerosols from the LBA-SMOCC campaign in Rondônia, Brazil. *Journal of Aerosol Science* **41**, 118–133. doi:10.1016/j.jaerosci.2009.08.006

Kuo LJ, Louchouarn P, Herbert BE (2011) Influence of combustion conditions on yields of solvent-extractable anhydrosugars and lignin phenols in chars: implications for characterizations of biomass combustion residues. *Chemosphere* **85**, 797–805. doi:10.1016/j.chemosphere.2011.06.074

Landis MS, Edgerton ES, White EM, Wentworth GR, Sullivan AP, Dillner AM (2018) The impact of the 2016 Fort McMurray Horse River Wildfire on ambient air pollution levels in the Athabasca Oil Sands Region, Alberta, Canada. *Science of the Total Environment* **618**, 1665–1676. doi:10.1016/j.scitotenv.2017.10.008

Landis MS, Long RW, Krug J, Colón M, Vanderpool R, Habel A, Urbanski SP (2021) The U.S. EPA wildland fire sensor challenge: performance and evaluation of solver submitted multi-pollutant sensor systems. *Atmospheric Environment* **247**, 118165. doi:10.1016/j.atmosenv.2020.118165

Laskin A, Smith JS, Laskin J (2009) Molecular characterization of nitrogen-containing organic compounds in biomass burning aerosols using high-resolution mass spectrometry. *Environmental Science and Technology* **43**(10), 3764–3771. doi:10.1021/es803456n

Li S, Liu D, Wu Y, Hu K, Jiang X, Tian P, Sheng J, Pan B, Zhao D (2023) Aging effects on residential biomass burning emissions under quasi-real atmospheric conditions. *Environmental Pollution* **337**, 122615. doi:10.1016/j.envpol.2023.122615

Liang Y, Jen CN, Weber RJ, Misztal PK, Goldstein AH (2021) Chemical composition of $PM_{2.5}$ in October 2017 Northern California wildfire plumes. *Atmospheric Chemistry and Physics* **21**, 5719–5737. doi:10.5194/acp-21-5719-2021

Liang Y, Stamatis C, Fortner EC, Wernis RA, Van Rooy P, Majluf F, Yacovitch TI, Daube C, Herndon SC, Kreisberg NM, Barsanti KC, Goldstein AH (2022) Emissions of organic compounds from western US wildfires and their near-fire transformations. *Atmospheric Chemistry and Physics* **22**, 9877–9893. doi:10.5194/acp-22-9877-2022

Liu JC, Mickley LJ, Sulprizio MP, Dominici F, Yue X, Ebisu K, Anderson GB, Khan RFA, Bravo MA, Bell ML (2016) Particulate air pollution from wildfires in the Western US under climate change. *Climatic Change* **138**, 655–666. doi:10.1007/s10584-016-1762-6

Malig BJ, Fairley D, Pearson D, Wu X, Ebisu K, Basu R (2021) Examining fine particulate matter and cause-specific morbidity during the 2017 North San Francisco Bay wildfires. *Science of the Total Environment* **787**, 147507. doi:10.1016/j.scitotenv.2021.147507

May AA, Levin EJT, Hennigan CJ, Riipinen I, Lee T, Collett JL, Jimenez JL, Kreidenweis SM, Robinson AL (2013) Gas-particle partitioning of primary organic aerosol emissions: 3. Biomass burning. *Journal of Geophysical Research: Atmospheres* **118**, 11327–11338. doi:10.1002/jgrd.50828

McClure CD, Jaffe DA (2018*a*) Investigation of high ozone events due to wildfire smoke in an urban area. *Atmospheric Environment* **194**, 146–157. doi:10.1016/j.atmosenv.2018.09.021

McClure CD, Jaffe DA (2018*b*) US particulate matter air quality improves except in wildfire-prone areas. *Proceedings of the National Academy of Sciences* **115**(31), 7901–7906. doi:10.1073/pnas.1804353115

McMurry PH, Rader DJ (1985) Aerosol wall losses in electrically charged chambers. *Aerosol Science and Technology* **4**, 249–268. doi:10.1080/02786828508959054

Miyazaki Y, Gowda D, Tachibana E, Takahashi Y, Hiura T (2019) Identification of secondary fatty alcohols in atmospheric aerosols in temperate forests. *Biogeosciences* **16**, 2181–2188. doi:10.5194/bg-16-2181-2019

Nestorowicz K, Jaoui M, Rudzinski KJ, Lewandowski M, Kleindienst TE, Spólnik G, Danikiewicz W, Szmigielski R (2018) Chemical composition of isoprene SOA under acidic and non-acidic conditions: effect of relative humidity. *Atmospheric Chemistry and Physics* **18**, 18101–18121. doi:10.5194/acp-18-18101-2018

Nikolić B, Todosijević M, Đorđević I, Stanković J, Mitić ZS, Tešević V, Marin PD (2020) Nonacosan-10-ol and *n*-Alkanes in Needles of *Pinus halepensis*. *Natural Product Communications* **15**(5), 1934578X2092097. doi:10.1177/1934578X20920970

Nolte CG, Schauer JJ, Cass GR, Simoneit BRT (2001) Highly polar organic compounds present in wood smoke and in the ambient atmosphere. *Environmental Science and Technology* **35**, 1912–1919. doi:10.1021/es001420r

Nozière B, Kalberer M, Claeys M, Allan J, D'anna B, Decesari S, Finessi E, Glasius M, Grgić I, Hamilton JF, Hoffmann T, Iinuma Y, Jaoui M, Kahnt A, Kampf CJ, Kourtchev I, Maenhaut W, Marsden N, Saarikoski S, SchnelleKreis J, Surratt JD, Szidat S, Szmigielski R, Wisthaler A (2015) The molecular identification of organic compounds in the atmosphere: state of the art and challenges. *Chemical Reviews* **115**, 3919–3983. doi:10.1021/cr5003485

Oros DR, Simoneit BRT (2001) Identification and emission factors of molecular tracers in organic aerosols from biomass burning Part 1. Temperate climate conifers. *Applied Geochemistry* **16**, 1513–1544. doi:10.1016/S0883-2927(01)00021-X

Otto A, Gondokusumo R, Simpson MJ (2006) Characterization and quantification of biomarkers from biomass burning at a recent wildfire site in Northern Alberta, Canada. *Applied Geochemistry* **21**(1), 166–183. doi:10.1016/j.apgeochem.2005.09.007

Ramdahl T (1983) Retene: a molecular marker of wood combustion in ambient air. *Nature* **306**, 580–582. doi:10.1038/306580a0

Schauer JJ, Kleeman MJ, Cass GR, Simoneit BRT (2001) Measurement of emissions from air pollution sources. 3. C_1–C_{29} organic compounds from fireplace combustion of wood. *Environmental Science & Technology* **35**, 1716–1728. doi:10.1021/es001331e

Shen X, Che H, Lv T, Wu B, Cao X, Li X, Zhang H, Hao X, Zhou Q, Yao Z (2023) Real-world emission characteristics of semivolatile/intermediate-volatility organic compounds originating from nonroad construction machinery in the working process. *Science of the Total Environment* **858**, 159970. doi:10.1016/j.scitotenv.2022.159970

Simoneit BRT (2002) Biomass burning: a review of organic tracers for smoke from incomplete combustion. *Applied Geochemistry* **17**, 129–162. doi:10.1016/S0883-2927(01)00061-0

Simoneit BRT, Rogge WF, Mazurek MA, Standley LJ, Hildemann LM, Cass GR (1993) Lignin pyrolysis products, lignans and resin acids as specific tracers of plant classes in emissions from biomass combustion. *Environmental Science and Technology* **27**, 2533–2541. doi:10.1021/es00048a034

Simoneit BRT, Schauer JJ, Nolte CG, Oros DR, Elias VO, Fraser MP, Rogge WF, Gass GR (1999) Levoglucosan, a tracer for cellulose in biomass burning and atmospheric particles. *Atmospheric Environment* **33**, 173–182. doi:10.1016/S1352-2310(98)00145-9

Standley LJ, Simoneit BRT (1994) Resin diterpenoids as tracers for biomass combustion aerosols. *Journal of Atmospheric Chemistry* **18**, 1–15. doi:10.1007/BF00694371

Stephens SL, Agee JK, Fulé PZ, North MP, Romme WH, Swetnam TW, Turner MG (2013) Managing forests and fire in changing climates. *Science* **342**(6154), 41–42. doi:10.1126/science.1240294

United States Environmental Protection Agency (U.S. EPA) (2016) 'Quality Assurance Guidance Document 2.12: monitoring PM2.5 in Ambient Air Using Designated Reference or Class I Equivalent Methods.' Publication No. EPA-454/B-16-001. (Office of Air Quality Planning and Standards Air Quality Analysis Division)

Urban RC, Alves CA, Allen AG, Cardoso AA, Queiroz MEC, Campos MLAM (2014) Sugar markers in aerosol particles from an agro-industrial region in Brazil. *Atmospheric Environment* **90**, 106–112. doi:10.1016/j.atmosenv.2014.03.034

Urbanski SP (2013) Combustion efficiency and emission factors for wildfire-season fires in mixed conifer forests of the northern Rocky Mountains, US. *Atmospheric Chemistry and Physics* **13**, 7241–7262. doi:10.5194/acp-13-7241-2013

Urbanski S (2014) Wildland fire emissions, carbon, and climate: emission factors. *Forest Ecology and Management* **317**, 51–60. doi:10.1016/j.foreco.2013.05.045

Vicente A, Alves C, Calvo AI, Fernandes AP, Nunes T, Monteiro C, Almeida SM, Pio C (2013) Emission factors and detailed chemical composition of smoke particles from the 2010 wildfire season. *Atmospheric Environment* **71**, 295–303. doi:10.1016/j.atmosenv.2013.01.062

Wang N, Jorga SD, Pierce JR, Donahue NM, Pandis SN (2018) Particle wall-loss correction methods in smog chamber experiments. *Atmospheric Measurement Techniques* **11**(12), 6577–6588. doi:10.5194/amt-11-6577-2018

Westerling ALR (2016) Increasing western US forest wildfire activity: sensitivity to changes in the timing of spring. *Philosophical Transactions of the Royal Society B* **371**, 20150178. doi:10.1098/rstb.2015.0178

Westerling AL, Hidalgo HG, Cayan DR, Swetnam TW (2006) Warming and earlier spring increase Western U.S. forest wildfire activity. *Science* **313**, 940–943. doi:10.1126/science.1128834

Xu J, Jia C, He J, Xu H, Tang Y-T, Ji D, Yu H, Xiao H, Wang C (2019) Biomass burning and fungal spores as sources of fine aerosols in Yangtze River Delta, China – using multiple organic tracers to understand variability, correlations and origins. *Environmental Pollution* **251**, 155–165. doi:10.1016/j.envpol.2019.04.090

Yan B, Zheng M, Hu YT, Lee S, Kim HK, Russell AG (2008) Organic composition of carbonaceous aerosols in an aged prescribed fire plume. *Atmospheric Chemistry and Physics* **8**(21), 6381–6394. doi:10.5194/acp-8-6381-2008

Data availability. Datasets related to this article can be found at https://catalog.data.gov/dataset/epa-sciencehub. doi:10.23719/1527910.

Conflicts of interest. The authors declare that they have no known competing financial interests or personal relationships that could have appeared to influence the work reported in this paper.

Declaration of funding. The EPA through its Office of Research and Development (ORD) funded and conducted this research.

Acknowledgements. The views expressed in this paper are those of the authors and do not necessarily reflect the views or policies of the EPA. It has been subjected to Agency review and approved for publication. Mention of trade names or commercial products do not constitute an endorsement or recommendation for use. The views, opinions, and findings contained in these works are those of the authors and should not be interpreted as an official US Forest Service or US Government position, policy, or decision.

Author contributions. Mohammed Jaoui: conceptualisation, methodology, validation, formal analysis, investigation, resources, data curation, writing – original draft, review and editing, visualisation. Shawn P. Urbanski: conceptualisation, methodology, validation, investigation, resources, visualisation, project administration. Russell W. Long: conceptualisation, methodology, validation, investigation, resources, data curation, writing – review and editing, project administration. Matthew S. Landis: conceptualisation, methodology, validation, investigation, resources, review and editing, visualisation, project administration, funding acquisition.

Author affiliations

[A]US Environmental Protection Agency (EPA), Office of Research and Development, Research Triangle Park, NC, USA.

[B]US Department of Agriculture (USDA), Forest Service, Rocky Mountain Research Station, Missoula, MT, USA.